

Articles

Synthesis and Photovoltaic Properties of Quinoxaline-Based Semiconducting Polymers with Fluoro Atoms

Suhee Song, Hyo Il Choi,[†] In Soo Shin, Hongsuk Suh,[‡] Myung Ho Hyun,[‡] Gun Dae Lee,[†]
Seong Soo Park,[†] Sung Heum Park,^{*} and Youngeup Jin^{†,*}*Department of Physics, Pukyong National University, Busan 608-739, Korea. *E-mail: spark@pknu.ac.kr**[†]Department of Industrial Chemistry, Pukyong National University, Busan 608-739, Korea. *E-mail: yjin@pknu.ac.kr**[‡]Department of Chemistry and Chemistry Institute for Functional Materials, Pusan National University, Busan 609-735, Korea**Received March 15, 2014, Accepted April 1, 2014*

A new acceptor unit, 6,7-difluoro-2,3-dihexylquinoxaline, was prepared and utilized for the synthesis of the conjugated polymers containing electron donor-acceptor pair for OPVs. New series of copolymers with dioctyloxybenzodithiophene as the electron rich unit and 6,7-difluoro-2,3-dihexylquinoxaline as the electron deficient unit are synthesized. The solid films of poly[2,6-(4,8-bis(2-ethylhexyloxy)benzo[1,2-*b*:4,5-*b'*]dithiophene)-*alt*-5,8-(6,7-difluoro-2,3-dihexylquinoxaline)] (**PBQxF**) and poly[2,6-(4,8-bis(2-ethylhexyloxy)benzo[1,2-*b*:4,5-*b'*]dithiophene)-*alt*-5,8-(6,7-difluoro-2,3-dihexyl-5,8-di(thiophen-2-yl) quinoxaline)] (**PBDTQxF**) show absorption bands with maximum peaks at about 599 and 551 nm and the absorption onsets at 692 and 713 nm, corresponding to band gaps of 1.79 and 1.74 eV, respectively. The devices comprising **PBQxF** with PC₇₁BM (1:2) showed open-circuit voltage (V_{OC}) of 0.64 V, short-circuit current density (J_{SC}) of 1.58 mA/cm², and fill factor (FF) of 0.39, giving power conversion efficiency (PCE) of 0.39%. To obtain absorption in the longer wavelength region, thiophene units without any alkyl group are incorporated as one of the monomers in **PBDTQxF**, which may result in low solubility of the polymers to lead lower efficiency.

Key Words : Polymer, OPVs, Synthesis, Fluoro

Introduction

Organic photovoltaics (OPVs) with bulk heterojunction (BHJ) architecture have become an active research area caused by promising alternative renewable energy source.^{1,2} Polymer solar cells offer the advantages, such as flexible, low-cost fabrication and lightweight plastic substrates.^{1,3,4} The development of novel materials is necessary to enhance the coverage of the solar spectrum and the absorption coefficients, which can improve the lower power-conversion efficiency and smaller photocurrent as compared to the case of inorganic solar cells.⁵ To achieve high efficiencies, the active layer of the polymer solar cells should have a broad and strong absorption in the range of solar spectrum.⁶ The HOMO and LUMO energy levels of the donor, such as lower bandgap conjugated polymer, and PCBM need to have optimal offset to maximize the attainable open circuit voltage (V_{OC}).⁷⁻⁹ Low-bandgap conjugated polymers which absorb in the red and near-IR region can better match the solar photon flux spectrum, which is important for the improvement of the OPV device performance through increases of the short-circuit current (J_{SC}).¹⁰

To obtain low bandgap conjugated polymers with planar molecular geometries, various types of aromatic heterocycles

have been widely investigated in OPVs.¹⁻⁶ Many of the low-bandgap (1.4-1.9 eV) conjugated polymers with excellent efficiencies have electron-deficient heterocycles, such as benzothiadiazole (BT),¹¹ quinoxaline¹² and benzimidazole,¹³ and electron-rich moieties, such as carbazole,^{14,15} thiophene,¹⁶ and benzodithiophene.¹⁷ The polybenzodithiophenes have been much emerged for organic solar cells caused by coplanarity, high hole mobility, and side chain patterns for enhanced solubility.^{18,19} Quinoxaline-based polymers have been much investigated to give high PCEs in solar cell applications.²⁰ Since F atom is anticipated to minimize the steric interactions, the introduction of electron-withdrawing F atom on the quinoxaline moieties is very attractive to lead planarization of the conjugated backbone.^{20,21} The fluorination of quinoxaline moieties have been reported to lead high efficiency caused by deeper HOMO, long wavelength absorption and high hole mobility.^{20,21}

New electron deficient unit, 6,7-difluoro-2,3-dihexylquinoxaline, has been designed and utilized for good solubility of organic solvent. In this study, we report new conjugated copolymers, **PBQxF** and **PBDTQxF** for OPV device utilizing a new type of acceptor, 6,7-difluoro-2,3-dihexylquinoxaline. To the absorption spectrum for the wider coverage of the solar spectrum, these donor-acceptor conjugated poly-

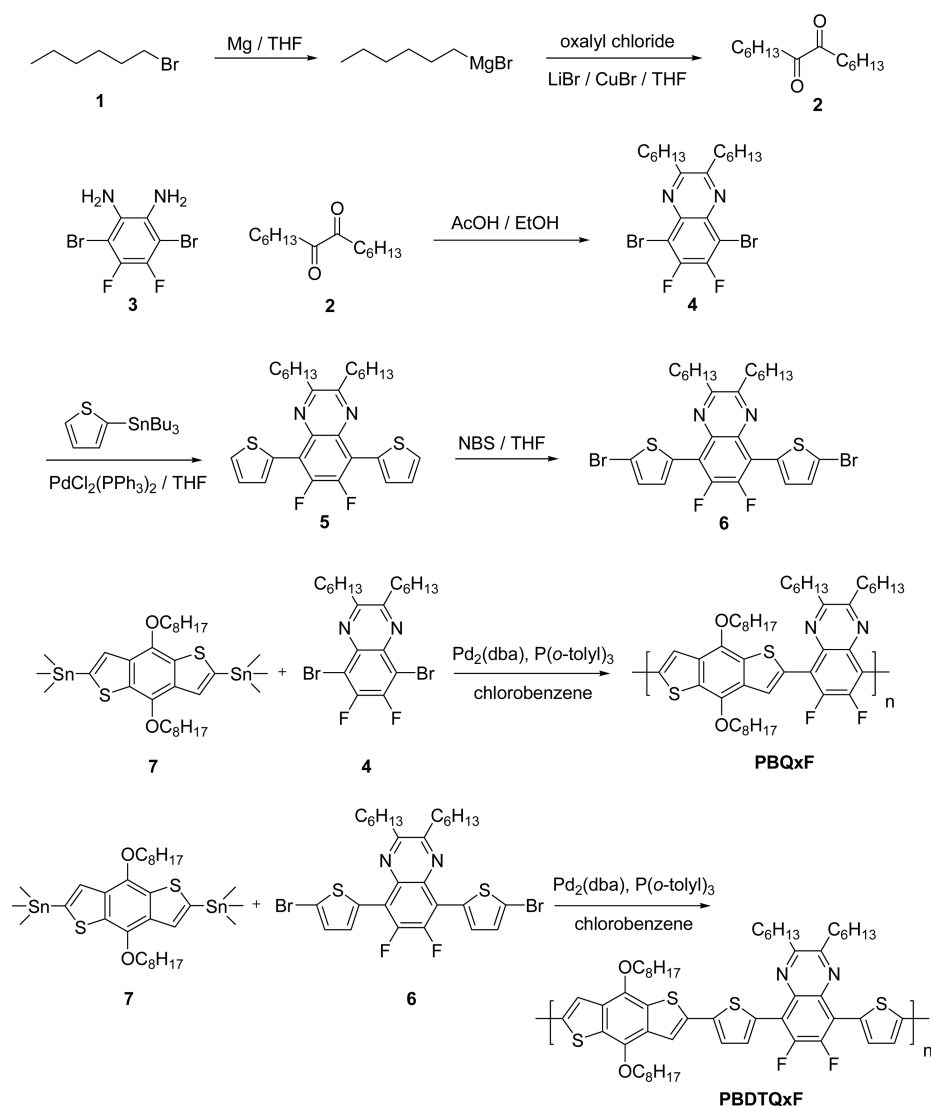
mers were synthesized by Stille coupling reaction of 2,6-bis(trimethyltin)-4,8-dioctyloxybenzo[1,2-*b*:3,4-*b'*]dithiophene and 5,8-dibromo-6,7-difluoro-2,3-dihexylquinoxaline (or 5,8-bis(5-bromothiophen-2-yl)-6,7-difluoro-2,3-dihexylquinoxaline). The photovoltaic properties of the polymers were investigated by fabrication of the polymer solar cells with the configuration of ITO/PEDOT:PSS/polymer:PCBM/Al.

Results and Discussion

Synthesis and Characterization. The general synthetic routes of the monomers and polymers are outlined in Scheme 1. In the first step, 3,6-dibromo-4,5-difluorobenzene-1,2-diamine (**3**) was cyclized with tetradecane-7,8-dione (**2**) to obtain 5,8-dibromo-6,7-difluoro-2,3-dihexylquinoxaline (**4**). Stille coupling reaction of 5,8-dibromo-6,7-difluoro-2,3-dihexylquinoxaline (**4**) with tributyl(2-thienyl)stannane were carried out to obtain 6,7-difluoro-2,3-dihexyl-5,8-di(thiophen-2-yl) quinoxaline (**5**). Compound **5** was brominat-

ed with *N*-bromosuccinimide (NBS) to generate 5,8-bis(5-bromothiophen-2-yl)-6,7-difluoro-2,3-dihexylquinoxaline (**6**). 2,6-Bis(trimethyltin)-4,8-dioctyloxybenzo[1,2-*b*:3,4-*b'*]dithiophene (**7**), as electron-rich moiety, and 5,8-dibromo-6,7-difluoro-2,3-dihexylquinoxaline (**4**) (or 5,8-bis(5-bromothiophen-2-yl)-6,7-difluoro-2,3-dihexylquinoxaline (**6**)) as electron-deficient moiety were copolymerized through Stille coupling polymerization with Pd(0)-catalyst to yield **PBQxF** (or **PBDTQxF**). The structures and purities of the monomers were confirmed by ¹H-NMR and HRMS. The synthesized polymer, **PBQxF**, was soluble in various organic solvents such as chloroform, chlorobenzene, THF, dichloromethane and *o*-dichlorobenzene (ODCB).

Table 1 summarized the polymerization results including molecular weight, polydispersity index (PDI) and thermal stability of the polymers. **PBQxF** and **PBDTQxF** were determined by GPC to have weight-average molecular weights (M_w) of 15900 and 7600 with polydispersity indexes (PDI, M_w/M_n) of 1.6 and 1.9, respectively. The **PBDTQxF** has lower molecular weight caused by lower solubility of



Scheme 1. Synthetic route for the synthesis of the monomers and polymers.

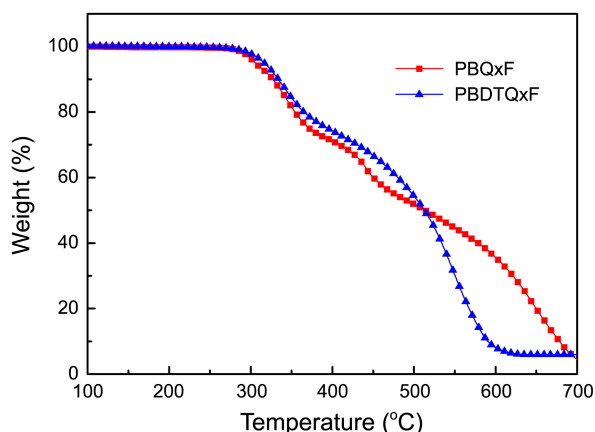
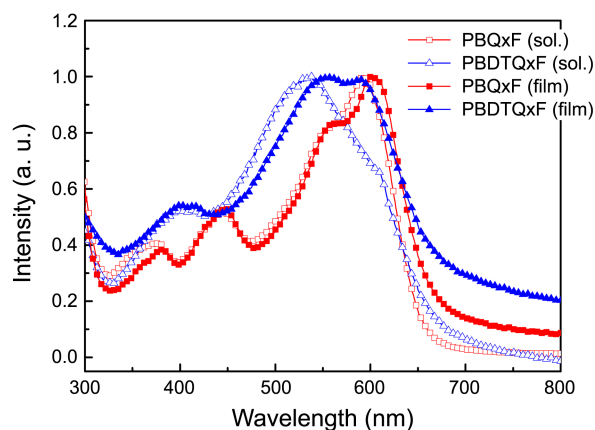
Table 1. Polymerization Results and Thermal Properties of Polymers

polymer	M_n^a (g/mol)	M_w^a (g/mol)	PDI ^a	TGA (T_d) ^b
PBQxF	9800	15900	1.6	305
PBDTQxF	4000	7600	1.9	316

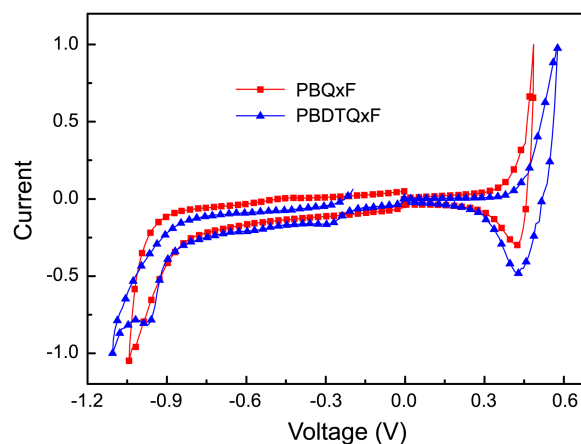
^aMolecular weight (M_w) and polydispersity (PDI) of the polymers were determined by gel permeation chromatography (GPC) in THF using polystyrene standards. ^bOnset decomposition temperature (5% weight loss) measured by TGA under N_2 .

chlorobenzene during synthesis process. The thermal properties of the polymers were characterized by thermal gravimetric analysis (TGA) as shown in Figure 1. Thermal gravimetric analysis was performed with TGA 2950 in a nitrogen atmosphere at a heating rate of 10 °C/min to 600 °C. The DSC analysis was performed under a nitrogen atmosphere (50 mL/min) on a DSC 2920 at heating rates of 10 °C/min. The decomposition temperatures (T_d) for **PBQxF** and **PBDTQxF** under N_2 were determined to be 305 and 316 °C, respectively. The T_d of **PBDTQxF** was higher than that of **PBQxF** caused by rigid thiophene unit. The glass transition temperatures of **PBQxF** and **PBDTQxF** were not measured in the range of 30–250 °C caused by longer alkyl chain on quinoxaline. The high thermal stability of the synthesized polymer prevents the deformation of the morphology and is important for OPV device applications.

Optical Properties. The optical properties of chloroform solution and films of the polymers were investigated by UV-vis absorption spectroscopy. Uniform films were prepared on quartz plate by spin-casting from their ODCB solution at room temperature. The absorption spectra of **PBQxF** and **PBDTQxF** exhibited maximum peaks at about 593 and 538 nm in solution, respectively. The solid films of **PBQxF** and **PBDTQxF** show absorption bands with maximum peaks at about 599 and 551 nm and the absorption onsets at 692 and 713 nm, corresponding to band gaps of 1.79 and 1.74 eV, respectively. The absorption spectra of the polymers are known to be related to their effective conjugation length.²² The absorption spectra of **PBDTQxF** with thiophene units were blue shifted as compared with **PBQxF** caused by lower molecular weight.

**Figure 1.** Thermogravimetric analysis of the polymers under N_2 .**Figure 2.** UV-visible absorption spectra of polymers in ODCB solution and the solid state.

Electrochemical Properties. The electrochemical properties of the polymers were determined from the band gap, which was estimated from the absorption onset wavelength and the HOMO energy level which was estimated from cyclic voltammetry (CV). The CV was performed with a solution of tetrabutylammonium tetrafluoroborate (Bu_4NBF_4) (0.10 M) in acetonitrile at a scan rate of 100 mV/s at room temperature under argon atmosphere. A platinum electrode (~ 0.05 cm²) coated with a thin polymer film was used as the working electrode. Pt wire and Ag/AgNO₃ electrode were used as the counter electrode and reference electrode, respectively. The energy level of the Ag/AgNO₃ reference electrode (calibrated by the Fc/Fc⁺ redox system) was 4.8 eV below the vacuum level. The CV spectra are shown in Figure 3, and the oxidation potentials derived from the onsets of electrochemical p-doping are summarized in Table 3. The HOMO and LUMO levels were calculated according to the empirical formula ($E_{HOMO} = -([E_{onset}]^{ox} + 4.8)$ eV) and

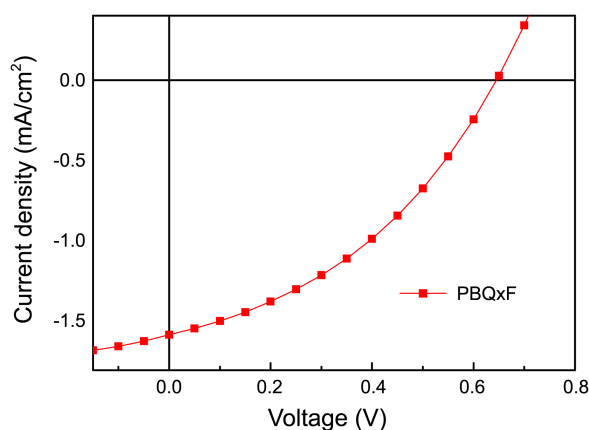
**Figure 3.** Electrochemical properties of polymers.**Table 2.** Characteristics of the UV-vis Absorption Spectra

polymer	in solution (nm)	in thin film (nm)
PBQxF	593	599
PBDTQxF	538	551

Table 3. Electrochemical Potentials and Energy Levels of the Polymers

polymers	optical band gap ^a (eV)	HOMO ^b (eV)	LUMO ^c (eV)	E_{ox}^d (V)	E_{red}^d (V)	electrochemical band gap ^e (eV)
PBQxF	1.79	-5.17	-4.00	0.37	-0.80	1.17
PBDTQxF	1.74	-5.22	-3.99	0.42	-0.81	1.23

^aOptical energy band gap was estimated from the onset wavelength of the optical absorption. ^bCalculated from the oxidation potentials. ^cCalculated from the reduction potentials. ^dOnset oxidation and reduction potential measured by cyclic voltammetry. ^eCalculated from the E_{ox} and E_{red} .

**Figure 4.** Current density-potential characteristics of the **PBDTQxF** solar cells under the illumination of AM 1.5, 100 mW/cm².

($E_{LUMO} = -([E_{onset}]^{red} + 4.8)$ eV), respectively. The band gaps of the **PBQxF** and **PBDTQxF** in thin films were determined to be 1.79 and 1.74 eV, which was calculated from the absorption onset wavelengths of 692 and 713 nm, respectively. The polymers exhibited irreversible processes in oxidation scans. The oxidation onsets of the **PBQxF** and **PBDTQxF** were estimated to be 0.37 and 0.42 V, which correspond to HOMO energy levels of -5.17 and -5.22 eV, respectively. The reduction onsets of the **PBQxF** and **PBDTQxF** were estimated to be -0.80 and -0.81 V, which correspond to LUMO energy levels of -4.00 and -3.99 eV, respectively. The electrochemical band gaps, calculated from cyclic voltammetry data, were determined to be 1.17 and 1.23 eV, which are lower than the optical band gaps estimated from the absorption spectra.

Polymer Photovoltaic Properties. The photovoltaic properties of polymers were investigated by fabricating the OPVs with ITO as positive electrode, the blend with small molecules and PCBM as active layer, and Al as negative electrode. Figure 4 showed the current-voltage (I - V) curves of the OPVs with the configuration of ITO/PEDOT:PSS (40 nm)/polymer:PC₇₁BM (100 nm)/Al (100 nm) under AM 1.5G irradiation (100 mW/cm²) and summarized in Table 4.

Table 4. Photovoltaic Properties of the Polymer Solar Cells

polymers	V_{oc} (V)	J_{sc} (mA/cm ²)	FF	PCE (%)
PBQxF	0.64	1.58	0.39	0.394
PBDTQxF	0.25	0.007	0.14	0.002

BHJ devices were fabricated by spin-coating of 1% (w/v) ODCB solutions comprising blend of polymers and PC₇₁BM. The devices comprising **PBQxF** with PC₇₁BM (1:2) showed open-circuit voltage (V_{oc}) of 0.64 V, short-circuit current density (J_{sc}) of 1.58 mA/cm², and fill factor (FF) of 0.39, giving a power conversion efficiency (PCE) of 0.39%. The device of **PBDTQxF**:PC₇₁BM (1:2) showed V_{oc} value of 0.25 V, J_{sc} value of 0.007 mA/cm², and FF of 0.14, giving PCE of 0.002%. The device performance of **PBDTQxF** was not worked caused by lower molecular weight.

Conclusions

New polymers, **PBQxF** and **PBDTQxF** utilizing 6,7-difluoro-2,3-dihexylquinoxaline, were synthesized at room temperature in organic solvents. The absorption spectra of **PBQxF** and **PBDTQxF** exhibited maximum peaks at about 593 and 538 nm in solution, respectively. The solid films of **PBQxF** and **PBDTQxF** show absorption bands with maximum peaks at about 599 and 551 nm and the absorption onsets at 692 and 713 nm. The devices comprising **PBQxF** with PC₇₁BM (1:2) showed V_{oc} of 0.64 V, J_{sc} of 1.58 mA/cm², and FF of 0.39, giving PCE of 0.39%.

Experimental Section

General. All reagents were purchased from Aldrich or TCI, and used without further purification. Solvents were purified by normal procedure and handled under moisture-free atmosphere. ¹H and ¹³C NMR spectra were recorded with a JNM ECP-400 (400 MHz, JEOL) spectrometer and chemical shifts were recorded in ppm units with TMS as the internal standard. Flash column chromatography was performed with Merck silica gel 60 (particle size 230-400 mesh ASTM) with ethyl acetate/hexane or methanol/methylene chloride gradients unless otherwise indicated. Analytical thin layer chromatography (TLC) was conducted using Merck 0.25 mm silica gel 60F pre-coated aluminum plates with fluorescent indicator UV254. High resolution mass spectra (HRMS) were recorded on a JEOL JMS-700 mass spectrometer under electron impact (EI) conditions in the Korea Basic Science Institute (Daegu). Molecular weight and polydispersity of the polymer were determined by gel permeation chromatography (GPC) analysis with a polystyrene standard calibration. The UV-vis absorption spectra were recorded by a Varian 5E UV/VIS/NIR spectrophotometer, while the Oriel InstaSpec IV CCD detection system with xenon lamp was used for the photoluminescence and electroluminescence.

science spectra measurements.

Solar cells were fabricated on an indium tin oxide (ITO)-coated glass substrate with the following structure; ITO-coated glass substrate/poly(3,4-ethylenedioxythiophene):poly(styrenesulfonate) (PEDOT:PSS)/polymer: PC₇₁BM/Al. The ITO-coated glass substrate was first cleaned with detergent, ultrasonicated in acetone and isopropyl alcohol, and subsequently dried overnight in an oven. PEDOT:PSS (Baytron PH) was spin-casted from aqueous solution to form a film of 40 nm thickness. The substrate was dried for 10 min at 140 °C in air and then transferred into a glove box to spin-cast the charge separation layer. A solution containing a mixture of polymer:PC₇₁BM in ODCB solvent with concentration of 7 wt/mL % was then spin-casted on top of the PEDOT/PSS layer. The film was dried for 60 min at 70 °C in the glove box. The sample was heated at 80 °C for 10 min in air. Then, an aluminum (Al, 100 nm) electrode was deposited by thermal evaporation in a vacuum of about 5×10^{-7} Torr. Current density-voltage (*J-V*) characteristics of the devices were measured using a Keithley 236 Source Measure Unit. Solar cell performance was measured by using an Air Mass 1.5 Global (AM 1.5 G) solar simulator with an irradiation intensity of 1000 Wm⁻². An aperture (12.7 mm²) was used on top of the cell to eliminate extrinsic effects such as crosstalk, waveguiding, shadow effects etc. The spectral mismatch factor was calculated by comparison of solar simulator spectrum with AM 1.5 spectrum at room temperature.

Synthesis of 5,8-Dibromo-6,7-difluoro-2,3-dihexylquinoxaline (4). A solution of tetradecane-7,8-dione (**2**) (1.8 mL, 7.95 mmol), 3,6-dibromo-4,5-difluorobenzene-1,2-diamine (**3**) (2.03 g, 6.62 mmol), and ethanol (150 mL) was heated at 70 °C overnight. After cooling to room temperature, the reaction mixture was treated with water and ethyl acetate. The aqueous phase was extracted with ethyl acetate and combined organic layer was dried with MgSO₄. After concentration of the organic phase under reduced pressure, the residue was purified by column chromatography to give compound **4** as white solid. ¹H NMR (400 MHz, CDCl₃) δ 0.89 (t, 6H, *J* = 7.0 Hz), 1.33-1.40 (m, 12H), 1.88 (quin, 4H, *J* = 7.8 Hz), 3.04 (t, 4H, *J* = 7.5 Hz). ¹³C NMR (100 MHz, CDCl₃) δ 14.06, 22.60, 27.43, 29.12, 31.73, 34.57, 109.15, 135.61, 149.5 (d, *J* = 254 Hz, C-F), 158.03. HRMS (*m/z*, EI⁺) calcd for C₂₀H₂₆Br₂F₂N₂ 490.0431, found 490.0435.

Synthesis of 6,7-Difluoro-2,3-dihexyl-5,8-di(thiophen-2-yl) quinoxaline (5). A solution of 5,8-dibromo-6,7-difluoro-2,3-dihexylquinoxaline (**4**) (5.63 g, 11.44 mmol) and tributyl(2-thienyl)stannane (17.08 g, 6.42 mmol) in 250 mL of THF at room temperature was treated with dichlorobis(triphenylphosphine)palladium(II) (2 mol %). The reaction mixture was stirred for 12 h at 110 °C, concentrated under reduced pressure, and the residue was purified by flash column chromatography to give compound **5** as a red solid. ¹H NMR (400 MHz, CDCl₃) δ 0.89 (t, 6H, *J* = 7.0 Hz), 1.35-1.48 (m, 12H), 1.97 (quin, 4H, *J* = 7.7 Hz), 3.07 (t, 4H, *J* = 7.5 Hz), 7.21 (d of d, 2H, *J* = 5.4 and 4.0 Hz), 7.59 (d, 2H, *J* = 5.4 Hz), 7.99 (d, 2H, *J* = 3.8 Hz). ¹³C NMR (100 MHz, CDCl₃) δ 14.10, 22.63, 27.88, 29.29, 31.78, 34.63, 117.24,

126.12, 129.37, 130.22, 130.99, 134.31, 148.68 (d, *J* = 255 Hz, C-F), 154.87.

Synthesis of 5,8-Bis(5-bromothiophen-2-yl)-6,7-difluoro-2,3-dihexylquinoxaline (6). 6,7-Difluoro-2,3-dihexyl-5,8-di(thiophen-2-yl) quinoxaline (**5**) (0.7 g, 1.4 mmol) was brominated with *N*-bromosuccinimide (NBS) (0.5 g, 2.8 mmol) in THF (10 mL) at room temperature. After stirring for 24 h, water (100 mL) and ethyl acetate (200 mL) were added. The organic phase was washed with 3×200 mL of water. The organic phase was concentrated under reduced pressure and the residue was purified by flash column chromatography to give compound **6** as a red solid. ¹H NMR (400 MHz, CDCl₃) δ 0.91 (t, 6H, *J* = 7.0 Hz), 1.38-1.48 (m, 12H), 1.98 (quin, 4H, *J* = 7.5 Hz), 3.09 (t, 4H, *J* = 7.5 Hz), 7.15 (d, 2H, *J* = 4.3 Hz), 7.75 (d, 2H, *J* = 4.3 Hz). ¹³C NMR (100 MHz, CDCl₃) δ 14.21, 22.59, 27.52, 29.42, 31.91, 34.88, 115.58, 118.52, 128.49, 129.68, 132.13, 132.45, 147.91 (d, *J* = 256 Hz, C-F), 154.50.

Polymerization of Poly[2,6-(4,8-bis(2-ethylhexyloxy)-benzo[1,2-*b*:4,5-*b'*]dithiophene)-*alt*-5,8-(6,7-difluoro-2,3-dihexylquinoxaline)] (PBQxF). Carefully purified 2,6-bis(trimethyltin)-4,8-dioctyloxybenzo[1,2-*b*:3,4-*b'*]dithiophene (**7**)²³ (628 mg, 0.81 mmol), 5,8-dibromo-6,7-difluoro-2,3-dihexylquinoxaline (**4**) (400 mg, 0.81 mmol), P(*o*-tolyl)₃ (40 mol %) and Pd₂(dba)₃ (5 mol %) were dissolved in 5 mL of chlorobenzene. The mixture was refluxed with vigorous stirring for 2 days under argon atmosphere. After cooling to room temperature, the mixture was poured into methanol. The precipitated material was recovered by filtration. The resulting solid material was reprecipitated using 100 mL of THF/1.0 L of methanol several times to remove residual amount of catalyst. The resulting polymer was soluble in THF, CHCl₃, ODCB and toluene.

Polymerization of Poly[2,6-(4,8-bis(2-ethylhexyloxy)-benzo[1,2-*b*:4,5-*b'*]dithiophene)-*alt*-5,8-(6,7-difluoro-2,3-dihexyl-5,8-di(thiophen-2-yl) quinoxaline)] (PBDTQxF). Carefully purified 2,6-bis(trimethyltin)-4,8-dioctyloxybenzo[1,2-*b*:3,4-*b'*]dithiophene (**7**) (647 mg, 0.84 mmol), 5,8-bis(5-bromothiophen-2-yl)-6,7-difluoro-2,3-dihexylquinoxaline (**6**) (550 mg, 0.84 mmol), P(*o*-tolyl)₃ (40 mol %) and Pd₂(dba)₃ (3 mol %) were dissolved in 5 mL of chlorobenzene. The mixture was refluxed with vigorous stirring for 2 days under argon atmosphere. After cooling to room temperature, the mixture was poured into methanol. The precipitated material was recovered by filtration. The resulting solid material was reprecipitated using 100 mL of THF/1.0 L of methanol several times to remove residual amount of catalyst. The resulting polymer was soluble in THF, CHCl₃, ODCB and toluene.

Acknowledgments. This work was supported by a Research Grant of Pukyong National University (2013 year: C-D-2013-0401).

References

1. Ko, S.; Mondal, R.; Risko, C.; Lee, J. K.; Hong, S.; McGehee, M.

- D.; Bredas, J. L.; Bao, Z. *Macromolecules* **2010**, *43*, 6685.
 2. Krieb, F. C.; Nielsen, T. D.; Fyenbo, J.; Wadström, M.; Pedersen, M. S. *Energy Environ. Sci.* **2010**, *3*, 512.
 3. Kim, J. Y.; Lee, K.; Coates, N. E.; Moses, D.; Nguyen, T.-Q.; Dante, M.; Heeger, A. J. *Science* **2007**, *317*, 222.
 4. Krebs, F. C.; Jørgensen, M.; Norrman, K.; Hagemann, O.; Alstrup, J.; Nielsen, T. D.; Fyenbo, J.; Larsen, K.; Kristensen, J. *Solar Energy Mater. Solar Cells* **2009**, *93*, 422.
 5. Scharber, M. C.; Muhlbacher, D.; Koppe, M.; Denk, P.; Waldauf, C.; Heeger, A. J.; Brabec, C. J. *Adv. Mater.* **2006**, *18*, 789.
 6. Hou, J.; Chen, H. Y.; Zhang, S.; Li, G.; Yang, Y. *J. Am. Chem. Soc.* **2008**, *130*, 16144.
 7. Xiao, S.; Zhou, H.; You, W. *Macromolecules* **2008**, *41*, 5688.
 8. Thompson, B. C.; Frechet, J. M. J. *Angew. Chem., Int. Ed.* **2008**, *47*, 58.
 9. Scharber, M. C.; Wühlbacher, D.; Koppe, M.; Denk, P.; Waldauf, C.; Heeger, A. J.; Brabec, C. L. *Adv. Mater.* **2006**, *18*, 789.
 10. Colladet, K.; Nicolas, M.; Goris, L.; Lutsen, L.; Vanderzande, D. *Thin Solid Films* **2004**, *7*, 451.
 11. Karikomi, M.; Kitamura, C.; Ranaka, S.; Yamashita, Y. *J. Am. Chem. Soc.* **1995**, *117*, 6791.
 12. Dutta, P.; Park, H.; Lee, W. H.; Kang, I. N.; Lee, S. H. *Polym. Chem.* **2014**, *5*, 132.
 13. Song, S.; Jin, Y.; Park, S. H.; Cho, S.; Kim, I.; Lee, K.; Heeger, A. J.; Suh, H. *J. Mater. Chem.* **2010**, *20*, 6517.
 14. Park, S. H.; Roy, A.; Beaupre, S.; Cho, S.; Coates, N.; Moon, J. S.; Moses, D.; Leclerc, M.; Lee, K.; Heeger, A. J. *Nat. Photonics* **2009**, *3*, 297.
 15. Liu, C. L.; Tsai, J. H.; Lee, W. Y.; Chen, W. C.; Jenekhe, S. A. *Macromolecules* **2008**, *41*, 6952.
 16. Jeeva, S.; Lukyanova, O.; Karas, A.; Dadvand, A.; Rosei, F.; Perepichka, D. F. *Adv. Funct. Mater.* **2010**, *20*, 1661.
 17. Song, K. W.; Lee, T. H.; Ko, E. J.; Back, K. H.; Moon, D. K. *J. Poly. Sci. Poly. Chem.* **2014**, *52*, 1028.
 18. Pan, H.; Li, Y.; Wu, Y.; Liu, P.; Ong, B. S.; Zhu, S.; Xu, G. *Chem. Mater.* **2006**, *18*, 3237.
 19. Pan, H.; Wu, Y.; Li, Y.; Liu, P.; Ong, B. S.; Zhu, S.; Xu, G. *Adv. Funct. Mater.* **2007**, *17*, 3574.
 20. Iyer, A.; Bjorgaard, J.; Anderson, T.; Köse, M. E. *Macromolecules* **2012**, *45*, 6380.
 21. Chen, H. C.; Chen, Y. H.; Liu, C. C.; Chien, Y. C.; Chou, S. W.; Chou, P. T. *Chem. Mater.* **2012**, *24*, 4766.
 22. Goedel, W. A.; Somanathan, N. S.; Enkelmann, V.; Wegner, G. *Makromol. Chem.* **1992**, *193*, 1195.
 23. Son, H. J.; Wang, W.; Xu, T.; Liang, Y.; Wu, Y.; Li, G.; Yu, L. J. *J. Am. Chem. Soc.* **2011**, *133*, 1885.
-